NJC

Accepted Manuscript

This is an *Accepted Manuscript*, which has been through the Royal Society of Chemistry peer review process and has been accepted for publication.

Accepted Manuscripts are published online shortly after acceptance, before technical editing, formatting and proof reading. Using this free service, authors can make their results available to the community, in citable form, before we publish the edited article. We will replace this *Accepted Manuscript* with the edited and formatted *Advance Article* as soon as it is available.

You can find more information about *Accepted Manuscripts* in the Information for Authors.

Please note that technical editing may introduce minor changes to the text and/or graphics, which may alter content. The journal's standard Terms & Conditions and the Ethical guidelines still apply. In no event shall the Royal Society of Chemistry be held responsible for any errors or omissions in this *Accepted Manuscript* or any consequences arising from the use of any information it contains.

ROYAL SOCIETY OF CHEMISTRY

www.rsc.org/njc

Please do not adjust margins

Journal Name

ARTICLE

Received 00th January 20xx,

Accepted 00th January 20xx

DOI: 10.1039/x0xx00000x

www.rsc.org/

In Vitro Antiproliferative Activity of Palladium(II) Thiosemicarbazone Complexes and the Corresponding Functionalized Chitosan Coated Magnetite Nanoparticles

Wilfredo Hernández[a], Abraham. J. Vaisberg[b], Mabel Tobar [c,d], Melisa Álvarez [c,d], Jorge Manzur [c,d*], Yuri Echevarría[d,e*], Evgenia Spodine [d,e*]

This work reports the synthesis and characterization of palladium(II) complexes $Pd(L^1)_2$ (**1**), $Pd(L^2)_2$ (**2**), $Pd(L^3)_2$ (**3**) and $Pd(L^4)_2$ (**4**), where L^1H: 1-naphthaldehyde thiosemicarbazone; L^2H: 4-phenyl-(1-naphthaldehyde) thiosemicarbazone; L^3H: (2-hydroxy-1-naphthaldehyde) thiosemicarbazone; L^4H: 4-phenyl-1-(2-hydroxy-1-naphthaldehyde) thiosemicarbazone. All four complexes show *in vitro* antiproliferative activity against the following human tumor cell lines: H460, DU145, MCF-7, M14, HT-29, K562, HuTu 80. In particular $Pd(L^1)_2$ has the most potent activity for all the studied cell lines (IC_{50} ~ 1 μM), with the exception of H460. $Pd(L^2)_2$ is a promising candidate as pharmacological agent, since it presents a significant activity and is more innocuous than cisplatin against mouse fibroblast normal cells, 3T3. $Pd(L^4)_2$ is the complex which exhibits the lowest activity against the same cell lines (IC_{50} ~ 11 μM), being ten times lower than that of $Pd(L^1)_2$. These complexes were used to functionalize chitosan coated superparamagnetic magnetite nanoparticles with a metallic core of 11-13 nm, and the activity of these functionalized nanoparticles (NPs) against diverse human tumor cell lines was also tested. The nanoparticles, functionalized with $Pd(L^1)_2$, $Pd(L^3)_2$ and $Pd(L^4)_2$ show antiproliferative activity against DU-145, while those with $Pd(L^2)_2$, $Pd(L^3)_2$ and $Pd(L^4)_2$ against HuTu80.

Introduction

Thiosemicarbazones derivatives and their transition metal complexes have been shown to possess a wide variety of biological activities as antiviral, antimicrobial, anticancer, and antitumor agents[1-8]. Recently, *in vitro* studies of the platinum(II) and palladium(II) bis-chelate complexes M(L)Cl and ML_2 with (*N,N,S*) ligands derived from thiosemicarbazone against different human tumor cell lines showed that these metal complexes are more cytotoxic than their respective ligands[9-11]. The nature of the heteroatomic ring and the presence of the imine group (-N=CH-) are important factors in the inhibitory action against tumor cell growth[12]. Probably, the high cytotoxicity of these complexes may be related to the intercalation between pairs of DNA bases, or to the breaking of DNA strands[13,14].

In cancer treatment a targeted controlled delivery of the anticancer drugs is desirable to avoid the damage of the normal tissue. For biomedical applications superparamagnetic nanoparticles are preferred because they can be guided by an external magnetic field and do not retain any magnetism after removal of the magnetic field; thus preventing the spontaneous aggregation of the nanoparticles. For this purpose,

[a]Facultad de Ingeniería Industrial, Universidad de Lima, Lima 33, Perú. [b]Laboratorios de Investigación y Desarrollo, Facultad de Ciencias y Filosofía, Universidad Peruana Cayetano Heredia, Lima 31, Perú. [c]Facultad de Ciencias Físicas y Matemáticas, Universidad de Chile, Santiago, Chile. [d]Centro para el Desarrollo de la Nanociencia y la Nanotecnología (CEDENNA). Santiago, Chile. [e]Facultad de Ciencias Químicas y Farmacéuticas, Universidad de Chile, Santiago, Chile.

e-mail: jmanzur@ing.uchile.cl, espodine@uchile.cl, yuriech@yahoo.es

Supplementary information. CCDC 966873 contains the supplementary crystallographic data for this paper. These data can be obtained free of charge at www.ccdc.cam.ac.uk/conts/retrieving.html [or from the Cambridge Crystallographic Data Centre (CCDC), 12 Union Road, Cambridge CB2 1EZ, UK; fax: +44(0)1223-336033; email: deposit@ccdc.cam.ac.uk].

New Journal of Chemistry Accepted Manuscript

Please do not adjust margins

superparamagnetic iron oxides are emerging as promising candidates because they can be obtained at nanoscale size and their biocompatibility has been proved[15-17]. Iron oxide nanoparticles have a great potential for several applications in medicine[16,17] including drug delivery[18,19] and hyperthermia[20]. For the improvement of targeting and biocompatibility the nanoparticles are coated with different species, which also allow further functionalization. Among others, chitosan is an interesting choice due to many significant biological (biodegradable, biocompatible, bioactive) and chemical properties (polycationic, hydrogel, contains reactive groups such as OH and NH)[20,21]. Kim et al.[22] reported chitosan-coated magnetic nanoparticles for application in magnetic targeted hyperthermia, where a temperature rise of 23°C under an alternating magnetic field can be obtained. The nanoparticles were biocompatible and exhibited higher affinity for KB carcinoma cells than L929 normal cells. The development of an embolic material capable of MRI contrast enhancement, based on microspheres obtained from superparamagnetic magnetite nanoparticles and chitosan has also been reported[23]. Besides, chitosan is characterized by its high affinity for metal ions and also can bind metal complexes[24,25].

In this work we describe the synthesis and characterization of thiosemicarbazone based palladium(II) complexes, based on ligands with shown anticancer properties, and the adsorption of compounds $(PdL^{1-4})_2$ on superparamagnetic magnetite nanoparticles coated with chitosan. A study of the antiproliferative activity of the above mentioned palladium(II) complexes, and that of the corresponding functionalized nanoparticles with $Pd(L^{1-4})_2$ is reported.

Experimental

Equipment

Palladium analyses for the complexes were carried out on an AAnalyst 700 Perkin Elmer equipment, using an acetylene/air flame. The analyses of C, N, and H were done on a Thermo Fisher Flash 2000 Elemental Analyzer. FT-IR spectra were registered using KBr pellets, on a Bruker Vector 22 equipment. ^{1}H-NMR spectra were obtained on a Bruker AMX-300 NMR spectrometer. X-ray powder diffraction was performed using a Bruker D-8 Advance diffractometer, with a CuKα1 radiation in the $5° < 2\theta < 60°$ range. The magnetic properties of the nanoparticles were measured at room temperature, on a vibrating magnetometer applying an external field from -10 T to 10 T. The average size of the core of the chitosan coated nanoparticles was estimated by the Debye-Scherrer formula[26]. The hydrodinamic average size of the functionalized nanoparticles was determined using a Zeta Sizer Nano ZS Malvern Instrument. A Milestone (Microwave Laboratory Systems) model LAVIS-1000 multiQUANT equipment was used to functionalize the coated nanoparticles. UV-visible spectra were obtained with a Lambda 11 Perkin Elmer spectrophotometer. TEM images were acquired on a FEI, Tecnai ST F20 microscope. Scanning electron microscopy (SEM) was done using a Jeol Scanning Microscope (JSM-5410), with an Oxford Link Isis energy dispersive X-ray detector (EDXS).

X-Ray Diffraction

X-ray data collection was made on a Bruker Smart Apex diffractometer, using separations of 0.3° between frames and 10 s by frame, at 293 K. Data integration was made using SAINTPLUS[27]. The structure of $Pd(L^2)_2 \cdot 4\,(C_3H_6O)$ (**2**) was solved by direct methods using XS in SHELXTL[28] and completed (non-H atoms) by Fourier difference synthesis. Refinement until convergence was obtained using XL SHELXTL and SHELXL97[29]. All hydrogen atoms were calculated in idealized positions on geometric basis, and refined with restrictions. Crystal data collection and refinement parameters for **2** are given in Table 1.

Synthesis of the ligands.

All reagents and solvents were Sigma-Aldrich of analytical quality, and were used without further purification. The ligands and complexes were prepared according to reported methods[30,31]. A solution of naphthaldehyde or 2-hydroxy-naphthaldehyde (20 mmol) in 40 mL of methanol was added to a hot solution of thiosemicarbazide (20 mmol) or 4-phenyl

New Journal of Chemistry Accepted Manuscript

This journal is © The Royal Society of Chemistry 20xx

Please do not adjust margins

thiosemicarbazide (20 mmol) in ethanol (100 mL). The reaction mixture was refluxed for 4 h and then stirred for 24 h at room temperature (scheme 1). The solid product was filtered, washed several times with cold ethanol or methanol, and dried *in vacuo*.

1-naphthaldehyde thiosemicarbazone (L^1H). Light yellow microcrystalline solid. Yield: 93%. Anal. Exp. % (calc. for $C_{12}H_{11}N_3S$): C: 62.7 (62.9), H: 4.7 (4.8), N: 18.4 (18.3). FTIR (KBr); ν(cm^{-1}): 3442, 3265 (NH_2), 3150 (NHCS), 1600 (C=N), 1110 (C=S). ^{1}H-NMR; (DMSO-d^6): 11.48 δ (s, 1H: =N-NH); 8.9 δ (s, 1H: N=C-H); 8.35 δ (d: 1H, H^8); 8.3 δ (s, br: 1H, NH_2); 8.2 δ (d, 1H: H^7); 7.95 δ (m, 3H: H^4, H^5; 1H, NH_2); 7.6 δ (m, 3H: H^3, H^6, H^7).

4-phenyl-(1-naphthaldehyde)-thiosemicarbazone (L^2H). Light yellow microcrystalline solid. Yield: 90%. Anal. Exp. % (calc. for $C_{18}H_{15}N_3S$): C: 70.5 (70.8), H: 4.9 (5.0), N: 13.7 (13.8). FTIR (KBr); ν(cm^{-1}): 3327 (NHPh), 3165 (NHCS), 1600 (C=N), 1088 (C=S). ^{1}H NMR (DMSO-d_6): 11.9 δ (s, 1H: =N-NH); 10.2 δ (s, 1H: NH-Ph); 9.05 δ (s, 1H: N=C-H); 8.45 δ (d, 1H: H^8); 8.3 (d, 1H: H^2): 8.0 δ (m, 2H: H^4, H^5); 7.57 δ (m, 5H: H^3, H^6, H^7; $2H_{ortho,}$ Ph); 7.38 δ (t, 2H: $2H_{meta}$, Ph); 7.24 δ (t, 1H: H_{para}, Ph).

(2-hydroxy-1-naphthaldehyde)thiosemicarbazone (L^3H). Yellow microcrystalline solid. Yield: 91%[31]. Anal. Exp. % (calc. for $C_{12}H_{11}N_3SO$): C: 58.5 (58.8), H: 4.4 (4.5), N: 16.9 (17.1). FTIR (KBr); ν (cm^{-1}): 3445, 3248 (NH_2), 3160 (NHCS), 1609 (C=N), 1114 (C=S). ^{1}H NMR (DMSO-d_6): 11.41 δ (s, 1H: =N-NH); 10.53 δ (s, br: 1H, OH); 9.05 δ (s, 1H: N=C-H); 8.51 δ (d: 1H, H^8); 8.22 δ (s, br: 1H, NH_2); 7.85 δ (m, 2H: H^4, H^5; 1H, NH_2); 7.56 δ (t, 1H: H^7); 7.36 δ (t, 1H, H^6); 7.19 δ (d, 1H, H^3).

4-Phenyl-1-(2-hydroxy-1-naphthaldehyde) thiosemi-carbazone, (L^4H). Intense yellow micro-crystalline solid. Yield: 90%. Anal. Exp. % (calc. for $C_{18}H_{15}N_3SO$): C: 67.5 (67.3), H: 4.6 (4.7), N: 12.8 (13.1). FTIR (KBr); ν (cm^{-1}): 3380 (NHPh), 3150 (NHCS), 1620 (C=N), 1084 (C=S). ^{1}H NMR (DMSO-d_6): 11.77 δ (s, 1H: =N-NH); 10.63 δ (s br: 1H, OH); 10.08 δ (s, 1H: NH-Ph); 9.17 δ (s, 1H: N=C-H); 8.49 δ (d, 1H: H^8); 7.89 δ (m, 2H: H^4, H^5); 7.57 δ (m, 3H: H^7; $2H_{ortho,}$ Ph); 7.38 δ (m, 3H, H^6; $2H_{meta}$, Ph); 7.24 δ (m, 2H, H^3; H_{para}, Ph).

Table 1 Crystal data and structure refinement for **2**

Empirical formula	$C_{48}\ H_{52}\ N_6\ O_4\ S_2\ Pd$
Formula weight	947.50
Temperature	297(2) K
Wavelength	0.71073 Å
Crystal system	Triclinic
Space group	P-1
Unit cell dimensions	a = 7.957(5) Å b = 9.112(5) Å c = 16.833(10) Å α= 80.061(9)° β= 80.638(9)° γ = 82.591(9)°
Volume	1179.7(12) Å3
Z	1
Density (calculated)	1.334 Mg/m^3
Absorption coefficient	0.530 mm-1
F(000)	492
Crystal size	0.40 x 0.31 x 0.11 mm^3
Theta range for data collection	2.28 to 27.96°
Index ranges	10<=h<=10, -11<=k<=11, -21<=l<=21
Reflections collected	9945
Independent reflections	5103 [R(int) = 0.0337]
Completeness to theta =	26.00° 98.7 %
Absorption correction	Semi-empirical from equivalents
Max. and min. transmission	0.943 and 0.821
Refinement method	Full-matrix least-squares on F^2
Data / restraints / parameters	5103 / 1 / 285
Goodness-of-fit on F2	1.035
Final R indices [I>2sigma(I)]	R_1 = 0.0594, wR_2 = 0.1462
R indices (all data)	R_1 = 0.0674, wR_2 = 0.1525
Largest diff. peak and hole	2.037 and -1.218 e.$Å^{-3}$

Synthesis of complexes.

General method.

A solution of $Pd(acac)_2$ (0.153 g, 0.5 mmol) in acetone-ethanol (2 : 1, 90 mL), was added dropwise to a stirred hot solution of L^nH (1.0 mmol) in ethanol (60 mL). Sodium acetate (0.082 g, 1 mmol) in 5 mL of water was then added. The solution was refluxed for 2 h and then stirred for 24 h at room temperature. (scheme 1). The precipitate was collected by filtration, washed three times with cold ethanol (50 mL) and dried under vacuum.

Bis[(1-naphthaldehyde)-thiosemicarbazonato] palladium(II), $Pd(L^1)_2$ (**1**). Orange microcrystalline solid. Yield: 91.8%. Anal. Exp. % (calc. for $C_{24}H_{20}N_6S_2Pd$): C:50.2 (51.2); N: 14.5 (14.9); H: 3.7 (3.6); Pd: 18.7 (18.9). FTIR (KBR); ν (cm^{-1}): 3440, 3330 (NH_2), 1600

New Journal of Chemistry Accepted Manuscript

Please do not adjust margins

(C=N), 1080 (C=S). ^{1}H-NMR; (DMSO-d^6): 8.15 δ (s, 1H: N=C-H); 8.60 δ (d: 1H, H^8); 8.05 δ (s, br: 2H, NH_2); 8.01 (d, 1H; H^4); 87.93 δ (d, 1H: H^2); 7.65 δ (various signals, 4H: H^3, H^5, H^6, H^7).

Bis[4-phenyl-(1-naphthaldehyde)thiosemicarbazonato]-palladium(II), Pd(L^2)$_2$·4 C_3H_6O (**2**). Orange micro-crystalline solid. Yield: 90.3%. Single crystals suitable for structure determination were obtained by recrystallization from acetone. Anal. Exp. % (calc. for $C_{48}H_{52}N_6S_2O_4Pd$): C:60.3 (60.8); N: 9.0 (8.9); H: 5.4 (5.5); Pd: 11.3 (11.2). FTIR (KBR); ν (cm^{-1}): 3380 (NHPh), 1594 (C=N), 1076 (C=S). ^{1}H-NMR; (DMSO-d^6): 8.46 δ (s, 1H: N=C-H); 8.27 δ (d: 1H, H^8); 9.90 δ (s, br: 1H, NH-Ph); 8.08; 8.12 δ (dd, 2H; H^4; H^5); 7.93 δ (d, 1H: H^2); 7.66 δ (various signals, 3H: H^6, H^7, *o*-H (Ph)); 7.26 δ (d, 1H; *o*-H (Ph)); 7.02 δ (t, 2 H; *m*-H (Ph); 6.96 δ (t, 1H, H3); 6.86 δ (t, 1H; *p*-H(Ph)).

Bis[(2-hydroxy-1-naphthaldehyde)thiosemicarbazonato] palladium(II), Pd(L^3)$_2$ (**3**). Orange micro-crystalline solid. Yield: 91.1%. Anal. Exp. % (calc. for $C_{24}H_{20}N_6S_2O_2Pd$): C:48.2 (48.4); N: 14.5 (14.1.); H: 3.5 (3.4); Pd: 17.7 (17.9). FTIR (KBr); ν (cm^{-1}): 3420, 3330 (broad, OH, NH_2), 1615 (C=N), 1092 (C=S) cm^{-1}. ^{1}H-NMR; (DMSO-d^6): 9.10, 8.95 δ (s, 2H: N=C-H); 8.80, 8.75 δ (d: 2H; H^8; H$^{8'}$); 10.25, 7.85, 6,70 δ (various signals, br: 4H; NH_2); 12.5, 10.75 δ (2H; OH; OH') 8.15, 7.95 δ (d, 2H; H^4, H$^{4'}$); 7.85 (m, 2H; H^5, H$^{5'}$),7.6, 7,5 δ (t, 2H; H^7, H$^{7'}$); 7.4 δ (t, 1H; H^3); 7.25 δ (m, 3H; H^6, H$^{6'}$, H$^{3'}$).

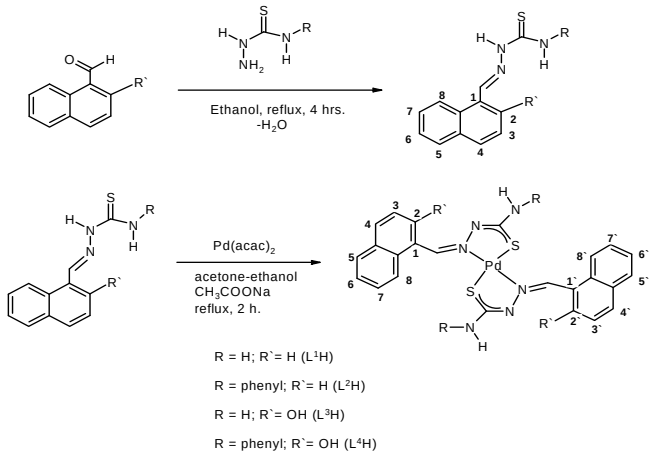

Scheme 1. Syntheses of ligands and complexes.

Bis[4-phenyl-(2-hydroxy-1-naphthaldehyde)thiosemi-carbazonato] palladium(II), Pd(L^4)$_2$ (**4**): Orange micro-crystalline solid. Yield: 90.8%. Anal. Exp. % (calc. for $C_{36}H_{28}N_6S_2O_2Pd$): C:58.1 (57.9); N: 11.5 (11.3.); H: 3.8 (3.8); Pd: 14.2 (14.3). FTIR (KBr); ν (cm^{-1}): 3400 (broad, OH, NH_2), 1592 (C=N), 1085 (C=S) cm^{-1}. ^{1}H-NMR; (DMSO-d^6): 9.35, 9.15 δ (s, 2H: N=C-H); 8.65, 8.35 δ (d: 2H; H^8; H$^{8'}$); 10.67, 9.50 δ (s, br: 2H; NH-Ph); 13.01, 10.95 δ (2H; OH; OH'); 7.85, 7.50, 7.30 δ (m, 18 H; arom protons); 6.95 δ (t, 2H; H^3, H$^{3'}$).

Chitosan coated magnetite nanoparticles.

A mixture of $FeCl_3 \cdot 6\ H_2O$ (2.7 g, 10 mmoles) and $FeCl_2 \cdot 4\ H_2O$ (1.0 g, 5 mmoles) in 50 mL of H_2O were stirred under nitrogen for 15 min. An aliquot of 12.5 mL of a degassed 1% solution of chitosan in 2% acetic acid was added, followed by the dropwise addition of 11.5 mL of a degassed 5 M NaOH solution, during 10 min. The nanoparticles were separated with a magnet, washed with water, acetone and dried under vacuum. Yield ca. 1.4 g.

Adsorption of Pd^{II} complexes on chitosan coated magnetite nanoparticles.

50 mg of coated magnetite nanoparticles and 5 mg of Pd(II) complex were dispersed in 20 mL of DMF by sonication at ambient temperature for 10 min.; the suspension was then irradiated with microwave (800 W) for 10 min. The particles were separated with a magnet and washed with 2-propanol and acetone and dried under vacuum. The adsorbed palladium(II) was determined by atomic absorption analyses, previous digestion of the particles in HNO_3. The calculated adsorption values are given in Table 2 as mg of adsorbed palladium complex for 100 mg of particles.

Biological activity

Cell culture

The BALB/3T3 (non-transformed mouse embryonic fibroblasts), were cultured in Dulbecco´s Modified Eagle Medium (DMEM) supplemented with 10 % newborn calf serum and 50 μg/mL gentamycin. H460

New Journal of Chemistry Accepted Manuscript

This journal is © The Royal Society of Chemistry 20xx

Please do not adjust margins

Table 2. Adsorption percentage of palladium(II) complexes on chitosan coated magnetite nanoparticles (100 mg of NPs).

Complex	$Pd(L^1)_2$	$Pd(L^2)_2$	$Pd(L^3)_2$	$Pd(L^4)_2$
Adsorption (%)	0.4	0.5	0.6	0.6

(human lung large cell carcinoma), DU145 (human prostate carcinoma) and HuTu 80 (human duodenum adenocarcinoma) cell lines were cultured in Eagle's Minimum Essential Medium (MEM) supplemented with 10 % fetal bovine serum and 50 μg/mL gentamycin. M-14 (human amelanotic melanoma), MCF-7 (human breast adenocarcinoma), HT-29 (human colon adenocarcinoma) and K562 (human chronic myelogenous leukemia) were cultured in RPMI 1640 Medium (RPMI) supplemented with 7.5 % fetal bovine serum and 50 μg/mL gentamycin in humidified 5 % CO_2 /95 % air at 37 °C.

Assessment of cytotoxicity

The assays were performed as described previously[30]. Briefly, 3000-5000 cells were inoculated in each well of 96-well tissue culture plates and incubated at 37 °C with their corresponding culture medium during 24 h. The palladium(II) complexes (0.01-10 μM) or cisplatin (1-10 μM) in DMSO were then added and incubated for 48 h at 37 °C with a highly humidified atmosphere, 5 % CO_2 and 95 % air. After the incubating period, cell monolayers were fixed with 10 % trichloroacetic acid and stained for 20 minutes, using the sulforhodamine B dye. Then, the excess dye was removed by washing repeatedly with 1 % acetic acid. The protein-bound dye was solubilized with 10 mM Tris buffer (pH 10.5) and the absorbance values were obtained at 510 nm, using a microplate reader. The IC_{50} value was defined as the concentration of a test sample resulting in a 50 % reduction of absorbance as compared with untreated controls, in other words 50% reduction in the growth of the cells, and was determined by linear regression analysis.

In the case of the cells treated with the functionalized nanoparticles with the palladium(II) complexes, after the 48 h of incubation and before adding the trichloroacetic acid to the cell monolayers, the growth media was removed and the plates were carefully washed twice with Hank's balanced salt solution in order to remove the nanoparticles that would otherwise interfere with the colorimetric assay . Then the cell monolayers were fixed with 10 % trichloroacetic acid and stained for 20 minutes, using the sulforhodamine B dye. The excess dye was removed by washing repeatedly with 1 % acetic acid. Then the protein-bound dye was solubilized with 10 mM Tris buffer (pH 10.5) and the absorbance values were obtained at 510 nm, using a microplate reader.

Results and discussion

The thiosemicarbazone ligands were obtained straightforwardly by reaction of the corresponding semicarbazide (R= H, phenyl) and substituted naphthaldehyde (R'=H, OH), while Pd^{II} complexes were synthesized by reaction of palladium(II) acetylacetonate with the corresponding thiosemicarbazone ligand. FTIR spectra of the complexes show the absorption bands corresponding to the C=N (*ca*. 1600 cm^{-1}) and C=S (*ca.* 1080 cm^{-1}) groups. For the ^{1}HNMR spectra, the =N-NH signal observed for the ligands at *ca*. 11-12 δ, is absent in the corresponding complexes due to the deprotonation on complexation. Besides, all complexes show the typical signal due to the N=C-H proton. The experimental results are in agreement with the expected compounds.

Structural description.

Recrystallization of the synthesized complexes in several solvents gave microcrystalline products. Only complex with HL^2, recrystallized from acetone, gave suitable crystals for X-ray diffraction studies. Complex $Pd(L^2)_2$ (**2**) crystallizes in the triclinic space group P-1 with one complex molecule and four acetone solvate molecules in the unit cell (Fig. 1).

New Journal of Chemistry Accepted Manuscript

Please do not adjust margins

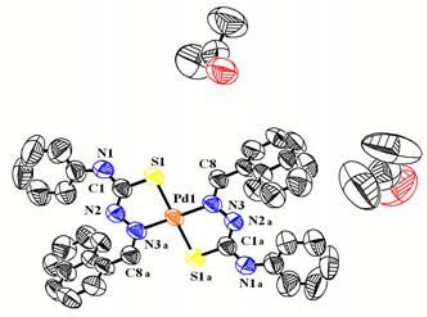

Figure 1. Graphical representation of **2**. Hydrogen atoms have been omitted for clarity.

The deprotonated ligand coordinates bidentately through the S and N atoms. The C7-N2 and C7-S1 bond distances are modified with respect to the free ligand, due to coordination[30]. The coordination of the Pd^{II} atom is square planar with a *trans* arrangement of the coordinating atoms. The angle formed by this plane with the mean phenyl plane is 20.24°, while the angle with the naphthalene mean plane is 66.60°. The phenyl and the naphthalene moieties are almost perpendicular, forming an angle of 78.69°. The N1-C1-N2-N3a-C8a moiety is planar with angles close to 120° (N1-C1-N2 = 120.0(3); C1-N2-N3a = 113.7(3) and N2-N3a-C8a = 114.8(3)°), according to the sp^2 character of the deprotonated N2 amine nitrogen. The Pd-S and the Pd-N distances are in the range of previously reported thiosemicarbazone derived complexes[30-33]. Selected bond lengths and angles are listed in Table 3.

Table 3. Selected bond lengths, (Å), and bond angles, (º), for $Pd(L^2)_2$ (**2**).

	Bond lengths Å		Bond angles (°)
Pd1-N3	2.029(3)	N3-Pd1-N3a	180.00(15)
Pd1-S1	2.2792(13)	N3-Pd1-S1	96.89(9)
S1-C1	1.732(4)	N3a-Pd1-S1	83.11(9)
C1-N2	1.308(4)	S1-Pd1-S1a	180
C1-N1	1.349(5)	C1-S1-Pd1	96.52(12)
N3a-N2	1.387(4)	N1-C1-N2	120.0(3)
C8-N3	1.287 (4)	C1-N2-N3a	113.7(3)
		N2-N3a-C8a	114.8(3)
		N1-C1-S1	114.9(3)
		C8-N3-Pd1	124.0(2)
		N2-N3a-Pd1	121.2(2)
		N2-C1-S1	125.1(3)

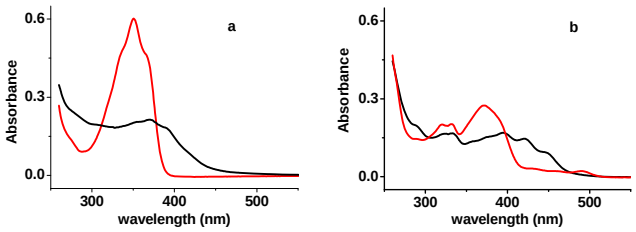

Figure 2. a) UV-Visible spectrum of L^1H (red) and $Pd(L^1)_2$ (black); b) L^4H (red) and $Pd(L^4)_2$ (black).

UV-visible spectra

Figure 2 shows the spectra of the selected ligands and the corresponding palladium(II) complexes. The spectra of the four ligands and the corresponding complexes can be classified in two groups: those that have the naphthaldehyde ring unsubstituted, bis [(1-naphthaldehyde) thiosemicarbazonato]palladium(II), $Pd(L^1)_2$ and bis[4-phenyl-(1-naphthaldehyde)-thiosemicarbazonato]palladium(II), $Pd(L^2)_2 \cdot 4\ C_3H_6O$ (**2**), and those which present a naphthaldehyde moiety substituted by a hydroxyl group,bis[(2-hydroxy-1-naphthaldehyde) thiosemicarbazonato]palladium(II), $Pd(L^3)_2$ (**3**) and bis[4-phenyl-(2-hydroxy-1-naphthaldehyde) thiosemicarbazonato]palladium(II), $Pd(L^4)_2$(4). As can be observed in the corresponding spectra, **1** and **2** are characterized by an absorption band that has a maximum at 370 nm and 354 nm, respectively, with shoulders at both higher and lower energies. When the spectra of **3** and **4** are analyzed it becomes evident that new absorption bands appear, making the spectra to have a more complex profile. At higher energies a double absorption band in the 325-350 nm region is observed for both **3** and **4**. At lower energies, in the 425 to 450 nm region another double absorption band is present. A similar effect has been reported for the spectra of naphthalene and 2-hydroxynaphthalene. The spectrum of 2-hydroxynaphthalene is characterized by a series of absorption maxima which are absent for naphthalene, compound that only absorbs below 300 nm[34]. Thus, it is possible to infer that the substitution of the naphtyl ring produces a set of new absorption bands, both at higher and lower energies, as compared with the intense band at 370 nm (**1**) or 350 nm (**2**), 375 nm (**3**)

New Journal of Chemistry Accepted Manuscript

This journal is © The Royal Society of Chemistry 20xx

Please do not adjust margins

and 380 nm (**4**). This band has been assigned to the n→ π* of the thiosemicarbazone group[35-37]. A detail of the bands and the corresponding log ϵ is given in Table S1.

The stability of the complexes in DMSO and DMSO/water solutions was controlled in order to have complete certainty that the species whose antiproliferative activity was recorded was the initial complex, and not a species derived from the decomposition of the initial complex. All recorded spectra at 24, 48, and 72 hours after the preparation of the solutions were similar to those obtained for the freshly prepared solutions.

Antiproliferative activity of the Pd^{II} complexes.

The cytotoxic potential of the synthesized palladium(II) complexes was investigated in the following six human tumor cell lines: DU145, MCF-7, H460, M14, HT-29, HuTu80 and K562. For comparison purposes, the cytotoxicity of the studied complexes was contrasted with that of the ligands and cisplatin, which were evaluated under the same experimental conditions[38]. The results of the cytotoxic activity of the ligands, palladium(II) complexes and cisplatin are expressed as IC_{50} values (micromolar concentration inhibiting 50 % cell growth), as shown in Table 4, and figure 3. The reported values are an average of three independent measurements, with a standard deviation of 10%.

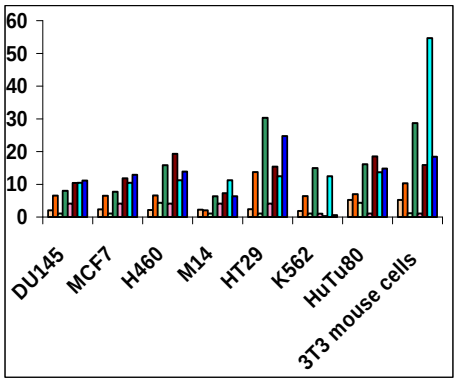

Figure 3. Citotoxic activity of complexes and the corresponding free ligans againts various tumor cell lines: $Pd(L^1)_2$; HL^1; $Pd(L^2)_2$; HL^2; $Pd(L^3)_2$; HL^3; $Pd(L^4)_2$; HL^4.

From the reported values of measured cytotoxic activities (Table 4), it is possible to infer that complex $Pd(L^1)_2$, (L^1H:1-naphtaldehyde thiosemicarbazone) has better activity in all cell lines than the original ligand. The same behavior is not observed for complex $Pd(L^2)_2$ since for both M14 and HuTu80 the activity of the complex and the ligand is similar (L^2H: 4-phenyl-(1-naphthaldehyde) thiosemicarbazone). Complex $Pd(L^3)_2$ (L^3H: (2-hydroxy-1-naphtaldehyde) thiosemicarbazone) has a better activity than that of the ligand, except in two cases: M14, where the activity in both is similar, and K562 where the activity of ligand is better than the corresponding complex. For complex $Pd(L^4)_2$, (L^4H: 4-phenyl-(2-hydroxy-1-naphthaldehyde)thiosemicarbaz-one) the activity of the complex and the ligand is similar for DU145, MCF7, HuTu80 and H460. When analyzing the data for M14 and K562, the activity of the ligand is better than that of the complex. Only for HT29 the activity of the complex becomes greater than that of the ligand. Even though $Pd(L^1)_2$ shows a better activity than $Pd(L^2)_2$ for most of the studied cell lines, $Pd(L^2)_2$ can be considered as the best of all the complexes according to the above cited cytotoxic activities, since it is more innocous than $Pd(L^1)_2$ against the studied normal cells. Moreover, when we compare the IC_{50} of this complex with that of cisplatin for all the studied cell lines, $Pd(L^2)_2$ is better than cisplatin with the exception of lines DU145, H460 and K562 cases where they have similar cytotoxic activities. Thus, this palladium(II) complex could be considered as a future candidate to be investigated as a pharmacological agent. As stated above, complex $Pd(L^4)_2$ is the least active of all the complexes, including the normal cells. However, when the activities between the complex and cisplatin are compared; in two cases the activity of the complex is better than that of cisplatin (MCF7 and HT29); is worse in four cases (DU145, H460, HuTu80 and K562), while $Pd(L^4)_2$ and cisplatin have similar activities for M14 line. So, striking differences in cytotoxicity were observed across the studied cell lines for the palladium species. All cell lines were consistently resistant to $Pd(L^4)_2$, while most were sensitive to $Pd(L^1)_2$, ($Pd(L^2)_2$ and $Pd(L^3)_2$.

New Journal of Chemistry Accepted Manuscript

Please do not adjust margins

Journal Name

ARTICLE

Table 4 Antiproliferative activity at 48 h, expressed in IC_{50} values. Values in parenthesis correspond to IC_{50} for pure ligands.

Human tumor cell lines / complex	$Pd(L^1)_2$ (L^1H)	$Pd(L^2)_2$ (L^2H)	$Pd(L^3)_2$ (L^3H)	$Pd(L^4)_2$ (L^4H)	Cisplatin
DU145	1.1 (8.0)	2.4 (26.5)	4.1 (10.4)	10.4 (11.2)	2.0
MCF7	1.1 (7.7)	2.1 (29.9)	<4.1 (11.8)	10.4(12.9)	19.8*
H460	4.3 (15.8)	2.1 (39.7)	4.1 (19.3)	11.3 (13.9)	1.5
M14	1.1 (6.4)	2.3 (>250)	4.1 (7.3)	11.3 (6.4)	8.5
HT29	1.1 (30.3)	2.4 (>250)	4.1 (15.4)	12.5 (24.7)	26.7
K562	1.1 (15.0)	1.8 (24.7)	1.0 (0.3)	12.5 (0.6)	1.1
HuTu80	4.4 (16.2)	5.2 (7.0)	1.1 (18.5)	13.7 (14.82)	7.6
3T3 mouse embryonic fibroblast cells	1.2 (28.7)	5.2 (10.3)	1.1 (16.0)	54.7(18.5)	2.1

*Palaniandavar et al[39] reported IC_{50} values for cisplatin using MCF-7.

These results permit to infer that the presence of the hydroxy substituent on the naphthaldehyde or the phenyl substituent on the thiosemicarbazone lowers the activity of the complexes by a factor of four and two approximately, as compared to the activity of the complex derived from the unsubstituted ligand.

In contrast, the presence of both substituents in the ligand decreases dramatically by a factor of ten the biological activity against all the studied tumor cell lines. With the exception of $Pd(L^4)_2$, all the studied complexes show similar or better biological activity than cisplatin. Thus, $Pd(L^4)_2$ shows the lowest biological activity as compared with the complex with the unsubstituted ligand or the ones which have either only the hydroxyl or the phenyl substituent.

A special reference has to be made in relation to the antiproliferative activity of $Pd(L^1)_2$ and $Pd(L^2)_2$ when tested with the MCF7 cell line (breast cancer). The activity of the studied complexes is much better than that of two recently reported Pd^{II} complexes with substituted diacetyl bis(^{4}N-tolylthiosemicarbazone) ligands[40].

The reported data does not permit to deduce a clear structure-activity correlation, since the antiproliferative activity of the complexes was shown to be sensitive to the type of cancer cell line used in the probes. While $Pd(L^1)_2$ has a planar naphtyl derived ligand, which would favour the intercalative interactions, the presence of phenyl rings does not enhance the antiproliferative activity of the studied complexes $Pd(L^2)_2$ and $Pd(L^4)_2$. This fact can be rationalized assuming that the presence of bulky phenyl groups, perpendicular to the

New Journal of Chemistry Accepted Manuscript

Please do not adjust margins

coordination plane, can sterically hinder the possible metal-DNA intercalation, thus lowering these interactions as compared with those of the palladium(II) complex with the unsubstituted, 1-naphthaldehyde thiosemicarbazone ligand, $Pd(L^1)_2$. Besides, apparently the hydrophobic phenyl groups present in the ligands of complexes **2** and **4** also do not enhance the permeability of these across the cell membrane, as could be expected. As the migration of the complexes into the cells by a concentration gradient is not increased, these complexes cannot increase their interference with the cellular function of DNA by binding to it.

Characterization of chitosan coated and functionalized magnetite nanoparticles.

Chitosan coated magnetite nanoparticles (NPs) were functionalized with the obtained palladium(II) complexes in order to investigate the possibility to use them as carriers for the studied drugs. These NPs can be directed to a specific site, where neoplastic cells exist, by an external magnetic field, since they can become superparamagnetic if a specific size is attained.

The average diameter of the metallic core of the coated nanoparticles was estimated by the Debye Scherrer formula, using the middle width of the highest peak of the corresponding diffraction pattern. The estimated average had a mean value of 10 nm (Fig. 4).

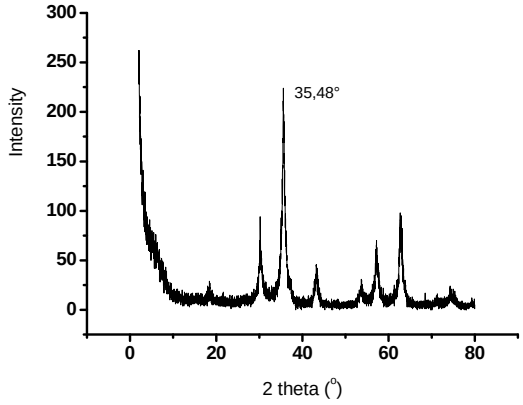

Figure 4. Powder X-raydiffractogram of coated magnetite nanoparticles.

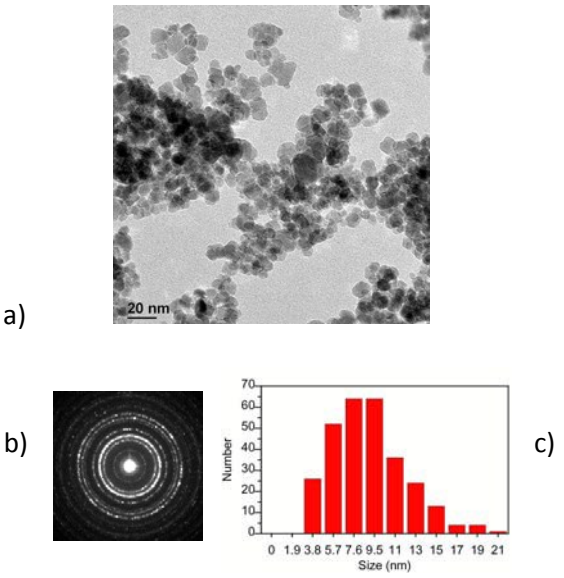

Figure 5. a) TEM image of coated nanoparticles, b) Diffraction pattern, c) Size distribution of the nanoparticles.

The cristallinity and size of these nanoparticles was corroborated by transmission electron microscopy (TEM), as shown in Fig. 5. Scanning electron microscopy images (SEM) are given for the chitosan coated nanoparticles as supplementary material (Fig. S2).The mean size permits to infer that the observed spherical particles correspond to agglomerates of the coated nanoparticles observed by TEM.

Figure 6 shows the magnetic behaviour of both the magnetite nanoparticles, and the coated magnetite ones. The curve corresponds to a typical superparamagnetic behaviour, since the coercivity is zero. The saturation magnetization is 50 emu/g for the pristine nanoparticles, while a lower value of 15 emu/g is obtained for the chitosan coated nanoparticles. These values are similar to those reported by Gupta et al. of 45 to 50 emu/g for nanoparticles of 12.92 nm[41].

From the obtained data the effect of the coating on the magnetic properties becomes evident. Several other authors have reported the decrease of the saturation magnetization of studied nanoparticles when these are coated, especially with organic polymers, since a non magnetic surface affects the magnetic behavior of the nanoparticles of size from 1 to 20 nm[42-46].

New Journal of Chemistry Accepted Manuscript

Please do not adjust margins

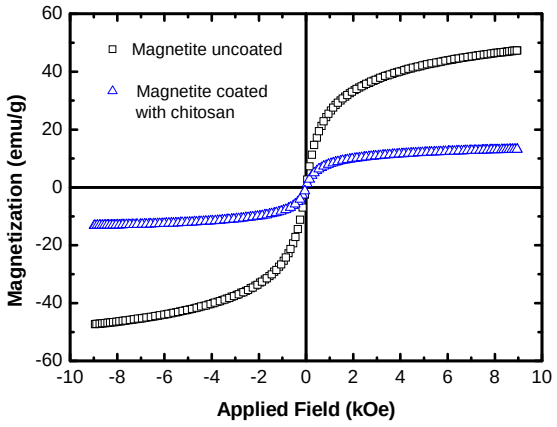

Figure 6. Magnetic properties of magnetite and coated magnetite nanoparticles.

The studied nanoparticles were then functionalized with the corresponding palladium(II) complexes. The hydrodynamic size of the functionalized nanoparticles was determined by the Dynamic Light Scattering technique (DLS). While the measured mean size of the chitosan coated nanoparticles was 300 nm, the functionalized nanoparticles were slightly smaller in size. The measured size for the $Pd(L^1)_2$, $Pd(L^2)_2$, $Pd(L^3)$ and $Pd(L^4)_2$ functionalized nanoparticles was in the range of 200 to 240 nm.

Table 5. *In vitro* antiproliferative activity of functionalyzed chitosan coated magnetite nanoparticles, expressed as percentages of remnant cancer cells.

Cell line	$Pd(L^1)_2$ (**1**)	$Pd(L^2)_2$ (**2**)	$Pd(L^3)_2$(**3**)	$Pd(L^4)_2$ (**4**)
DU-145	60	w/a	75	60
MCF7	w/a*	w/a	w/a	w/a
H460	w/a	w/a	w/a	w/a
M14	w/a	w/a	w/a	w/a
K562	w/a	w/a	50	w/a
HuTu80	w/a	76	25	75
3T3	w/a	w/a	w/a	w/a

* Without significant activity. (0.5 mg of nanoparticles/ml equivalent to *ca*. 4 μmoles of complex/ml).

Moreover, the electrokinetic potential changes for the chitosan coated nanoparticles as compared to that of the functionalized ones, from a negative value (-20 mV) to a positive one (range between 25 to 30 eV). This change can be attributed to the adsorption of the palladium complex on the chitosan surface. The electrokinetic potential for the coated nanoparticles is negative due to the fact that the amine groups of the chitosan are not protonated in the range of pH = 6; this value being the pH of the solutions where the measurements were done. This pH was larger than the isoelectric point for chitosan (pH = 5.45). The obtained results are similar to those reported by Zhang et al[47].

In vitro antiproliferative activity of functionalized chitosan coated magnetite nanoparticles.

All four complexes were used to functionalize the nanoparticles coated with chitosan. The NPs, whose palladium content was approximately 0.5 mg complex/100 mg of coated nanoparticles, were suspended in the same biological medium used to study the antiproliferative activity of the original thiosemicarbazone derived palladium(II) complexes. All experimental conditions were maintained constant, in order to obtain an estimation of the activity of the functionalized NPs. The results permitted to assess that the functionalized NPs present some activity against the DU145, K562 and HuTu80 tumor cell lines (Table 5).

The data of Table 5 indicate that the observed activity of the functionalized nanoparticles is not related to that of the free complexes. The adsorption process probably prevents the intercalation of the complex, thus reducing its activity. Moreover, it is possible to infer from the obtained data that the complexes are not liberated from the surface of the nanoparticles, during the study. The observed activity would be intrinsic to that of the functionalized nanoparticles.

New Journal of Chemistry Accepted Manuscript

This journal is © The Royal Society of Chemistry 20xx

Please do not adjust margins

Conclusions

In this work the antiproliferative activity of four ligands derived from thiosemicarbazone and the corresponding palladium(II) complexes was studied and compared to cisplatin.

Even though the activity of $Pd(L^1)_2$ is better than that of $Pd(L^2)_2$ the last one is more inocuous to normal cells, thus being a better candidate for pharmacological use. Both complexes have similar activity as compared to cisplatin, with the exception of MCF7, M14, HT29 cell lines. For these cell lines, the two studied complexes have a better antiproliferative activity.

The immobilization of the complexes on the surface of magnetite nanoparticles reduces the activity of the complexes. Some exceptions can be mentioned, for example, nanoparticles functionalized with $Pd(L^3)_2$ show activity against HuTu80, K562 and DU145.

Acknowledgements

W. H. thanks Universidad de Lima Scientific Research Institute for financial support. E. S., M. T., M.A. and J. M. thank Basal Project FB0807 (CEDENNA), and Y.E. thanks FONDECYT Project 3130418.

References

1 A. Gómez, C. Navarro, *Coord. Chem. Rev.,* 2004, **248**, 119.

2 K. S. Abou Melha, *J. Enz. Inhib. Medic. Chem.,* 2008, **23**, 493.

3 A. K. Salman, Y. Mohamad, *Eur. J. Med. Chem.,* 2009, **44**, 2270.

4 S. A. Elsayed, A. M. El-Hendawy, S. I .Mostafa, B. J. Jean-Claude, M. Todorova, I. S. Butler, *Bioinorg. Chem. Appl.*, 2010, ID 149149. DOI:10.1155/2010/149149.

5 M. Jagadeesh, H. K. Rashimi, Y. S. Rao, A. S. Reddy, B. Prathima, P. U. Maheswari, A. V. Reddy, *Spectrochim. Acta A,* 2013, **115**, 583.

6 C. Santini, M. Pellei, V. Gandin, M. Porchia, F. Tisato, C. Marzano, *Chem. Rev.,* 2014, **114**, 815.

7 S. A. Elsayed, I. S. Butler, F. R. Gilson, B. J. Jean-Claude, S. I. Mostafa, *J. Coord. Chem.,* 2014, **67**, 2711.

8 M. Jagadeesh, M. Lavanya, S. K. Kalangi, Y. Sarala, C. Ramachandraiah, A. V. Reddy, *Spectrochim. Acta A,* 2015, **135**, 180.

9 W. Hernández, J. Paz, J. Vaisberg, E. Spodine, R. Richter, L. Beyer, *Bioinorg. Chem. Appl.,* 2008, ID 690952.

10 D. Kovala-Demertzi, A. Papageorgiou, L. Papathanasis, A. Alexandratos, P. Dalezis, J. R. Miler, M. A. Demertzis, *Eur. J. Med. Chem.,* 2009, **44**, 1296.

11 Z. Iakovidou, A. Papageorgiou, M. A. Demertzis, E. Mioglou, D. Mourelatos, A. Kotsis, P. Nath Yadav, D. Kovala-Demertzi, *Anti-Cancer Drugs,* 2001, **12**, 65.

12 D. Kovala-Demertzi, M. A. Demertzis, J. R. Miller, C. Papadopoulou, C. Dodorou, G. Filousis, *J. Inorg. Biochem.,* 2001, **86**, 555.

13 I. H. Hall, C. B. Lackey, T. D. Klister, R. W. Durhman, E. M. Jouad, M. Khan , X. D. Thanh , S. Djebbar–Sid , O. Benali-Baitich, G. M. Bouet, *Pharmazie,* 2000, **55**, 937.

14 M. Baldini, M. Belicchi-Ferrari, F. Bisceglie, G. Pelosi, S. Pinelli, P. Tarasconi, *Inorg. Chem.,* 2003, **42**, 2049.

15 D. M. Souza, A. L. Andrade, J. D. Fabris, P. Valério, A. M. Goes, M. F. Leite, R. Z. Domingues, *J. Non-Cryst. Solids,* 2008, **354**, 4894.

16 C. C. Berry, A. S. G. Curtis, *J. Phys. D Appl. Phys.,* 2003, **36**, R198.

New Journal of Chemistry Accepted Manuscript

Please do not adjust margins

17 Q. A. Pankhurst, J. Connolly, S. K. Jones, J. Dobson, *J. Phys. D Appl. Phys.,* 2003, **36**, R167.

18 T. K. Jain, M. A. Morales, S. K. Sahoo, D. L. Leslie-Pelecky, V. Labhasetwar, *Molec. Pharm.,* 2005, **2**, 194.

19 Y. Zhang, N. Kohler, M. Zhang, *Biomater.,* 2002, **23**, 1553.

20 A. K. Gupta, M. Gupta, *Biomater.,* 2005, **26**, 3995.

21 S. R. Bhattarai, R. B. Kc, S. Y. Kim, M. Sharma, M. S. Khil, P. H. Hwang, G. H. Chung, H. Y. Kim, *J. Nanobiotech.,* 2008, **6**, 1.

22 D. H. Kim, K. N. Kim, K. M. Kim, Y. K. Lee, *J. Biomed. Mater. Res. A,* 2009, **88**, 1.

23 E. E. Kim, Y. Ahnb, H. S. Lee, *J. Alloys Compd.,* 2007, **434-435**, 633.

24 S. M. Nomanbhay, K. Palanisamy, *Electronic J. Biotech.,* 2005, **8**, 43.

25 R. Navarro, J. Guzmán, I. Saucedo, J. Revilla, E. Guibal, *Macromol. Biosci.,* 2003, **3**, 552.

26 A. L. Patterson, *Phys. Rev.,* 1939, **56**, 978.

27 *SAINTPLUS Version 6.02; Brucker AXS: Madison, WI,* 1999.

28 *SHELXTL Version 5.1; Brucker AXS : Madison, WI,* 1998.

29 G. M. Sheldrick, *SHELXL – 97; Program for Crystal Structure Refinement.* University of Gottingen, Germany, 1997.

30 W. Hernández, J. Paz, F. Carrasco, A. Vaisberg, E. Spodine, J. Manzur, L. Hennig, J. Sieler, S. Blaurock L. Beyer, *Bioinorg. Chem. Appl.,* 2013, ID 524701, http://dx.doi.org/10.1155/2013/524701.

31 W. Hernández, J. Paz, F. Carrasco, A. Vaisberg, J. Manzur, E. Spodine, L. Hennig, J. Sieler, L. Beyer, Z. *Naturforsh.,* 2010, **65 b**, 1271.

32 P. Skehan, R. Storeng, D. Scudiero, A. Monks, J. Mcmahon, D. Vistica, J. T. Warren, H. Bokesch, S. Kenney, M. R. Boyd, *J. Natl. Cancer Inst,* 1990, **82**, 1107.

33 R. Prabhakaran, P. Kalaivani, R. Huang, P. Poornima, V. Vijaya Padina, F. Dallemer, K. Natarajan, *J. Biol. Inorg. Chem.*, 2013, **18**, 233.

34 T. Che-Shung Lin ,W. C. Lin, *J. Chin. Chem. Soc.* 1961, **8**, 156.

35 D. Kovala-Demertzi, A. Domopoulou, M. A. Demertzi, G. Valle, A. Papageorgiou, *J. Inorg. Biochem., 1997, **68**,* 148.

36 N. Bharti, F. Athar, M. R. Maurya, A. Azam, *Bioorg. Med. Chem.,* 2004, **12**, 4679.

37 K. Husain, M. Abid, A. Azam, *Eur. J. Med. Chem*., 2008, **43**, 393.

38 A. I. Matesanz, C. Hernández, A. Rodriguez, P. Souza, *J. Inorg. Biochem.,* 2011, **105**, 1613.

39 M. Ganeshpandian, R. Loganathan, S. Ramakrishnan, A. Riyasdeen, M. A. Akbarsha, M. Palaniandavar, *Polyhedron,* 2013, **52**, 924.

40 A. I. Matesanz, I. Leitao, P. Souz, *J. Inorg. Biochem.,* 2013, **125**, 26.

41 A. K. Gupta, A. S. G. Curtis, *Biomater.,* 2004, **25**, 3029.

42 S. A. Gómez-Lopera, R. C. Plaza, A. V. Delgado, *J. Colloid Interf. Sci.,* 2001, **240**, 40.

43 W. Voit, D. K. Kim, W. Zapka, M. Muhammed, K. V. Rao, *Mater. Res. Soc., Symp. Proc.,* 2001, **676**, Y 7.8, 1.

44 Y. Li, P. Xiong, S. V. Molnar, S. Wirth, Y. Ohno, H. Ohno, *Appl. Phys. Lett.,* 2002, **80**, 4644.

45 D. H. Han, J. P. Wang, H. L. Luo, *J. Magn. Magn. Mater.,* 1994, **136**, 176.

New Journal of Chemistry Accepted Manuscript

This journal is © The Royal Society of Chemistry 20xx

Please do not adjust margins

46 F. Tourinho, R. Franck, R. Massart, R. Perzynski, *Prog. Colloid Polym. Sci.,* 1989, **79**, 128.

47 X. Zhang, R. Bai, *J. Colloid Interf. Sci.,* 2003, **264**, 30.

New Journal of Chemistry Accepted Manuscript

Please do not adjust margins

In Vitro Antiproliferative Activity of Palladium(II) Thiosemicarbazone Complexes and the Corresponding Functionalized Chitosan Coated Magnetite Nanoparticles

Wilfredo Hernandez, Abraham J.Vaisberg, Mabel Tobar, Melisa Alvarez,

Jorge Manzur, Yuri Echevarría, Evgenia Spodine

Magnetite functionalized nanoparticles with $Pd(L^3)_2$ and $Pd(L^4)_2$ show antiproliferative activity against DU-145 and HuTu80; $Pd(L^2)_2$ appears as promising pharmacological agent.

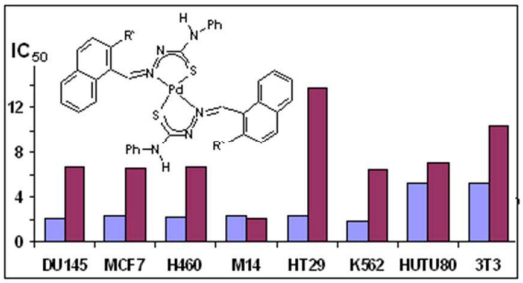

New Journal of Chemistry Accepted Manuscript